

Crystal structure, molecular docking and protective activity on myocarditis of Co(II) coordination polymer based nanoparticles

Dong-Song Bai^a, Li-Ying Bai^a, Ming Zhao^{a, b, **, *}, Qing-Shan Zhang^{a, b, *}

^a Inner Mongolia Key Laboratory of Mongolian Medicine Pharmacology for Cardio-Cerebral Vascular System, Tongliao, Inner Mongolia, 028000, China

^b Affiliated Hospital of Inner Mongolia University for Nationalities, Institute of Mongolia and Western Medicinal Treatment, Tongliao, Inner Mongolia, 028007, China

ARTICLE INFO

Article history:

Received 29 May 2019

Received in revised form

29 August 2019

Accepted 4 September 2019

Available online 5 September 2019

Keywords:

Coordination polymer

Myocarditis

Left ventricular ejection fraction

Molecular docking

ABSTRACT

This work presents the synthesis and characterization of a dicyanamide-bridged coordination polymer $[\text{Co}(\text{L})_2(\text{dca})]_n$ (**1**) by using the bidentate NO donor Schiff base ligand (2-methoxy-6-((methylimino)methyl)phenol). Furthermore, the nanoparticles of complex **1** (denoted as nano **1**) was prepared by a green grinding approach, which has good water dispersibility. The CVB3 infection mice model was built successfully, followed by nano **1** given for treatment. RT-PCR was used to detect the loading of CVB3 virus after nano **1** treatment. The left ventricular fractional shortening (LVFS) as well as left ventricular ejection fraction (LVEF) were assessed to evaluate the protective effect of cardiac functions after exposed to nano **1**. The toxicities of nano **1** on H9C2 and HL-1 cardiomyocytes was evaluated by CCK-8 assay. The hypothesis originated from the experimental observations has been further confirmed by using molecular docking simulation.

© 2019 Elsevier B.V. All rights reserved.

1. Introduction

As we all know, myocarditis is an autoimmune disease that leads to high death rate in the world every year [1]. It is a common heart disease with severe inflammatory immune infiltration and necrosis of myocardial cells. It can develop into chronic dilated cardiomyopathy (DCM) and cause sudden death [2,3]. Among different myocarditis, the viral myocarditis is the most common one, which is an inflammatory response usually resulted from the infection of myocardial virus, and the coxsackievirus B3 (CVB3) is the most familiar pathogen as reported [4]. Relying on the rearrangement of intracellular membranes into double-membrane vesicles, the replication of CVB3 explains the mechanism of viral myocarditis [5]. However, up to now, there is still no available efficient therapeutic agent against viral myocarditis.

Metal supramolecular structures and their design on the basis of

crystal engineering are the focus of research in the field of coordination chemistry supramolecular chemistry [6,7]. The more and more attention in this field is attributed to its valuable unit structure, as well as their latent applications in catalysis, biochemistry and luminescence, and especially in contemporary medicinal chemistry [8–12]. Because of its latent drug application value, functional complexes have attracted wide attention in these prepared complexes. And therefore, the selection of biocompatible ligands, safe and highly efficient has become a key element in the field of clinical practice, the structural design as well as drug treatment. Metal complexes containing oxygen and nitrogen ligands, such as Schiff base, have become more and more interest and current in the coordination chemistry field, due to many complexes have anticancer activity [13–16]. 4-chlorobenzaldehyde and 2-aminophenol bidentate Schiff base ligand have many biological and clinical applications. On the other hand, Cobalt is a necessary element of human body, indirectly regulates DNA synthesis in the active site of vitamin B12. Because of its remarkable biological activity, it attracts many organic metal chemists and biologists to study cobalt complexes with a view to their medical applications [17]. Because cobalt complexes have the ability of redox-dependent targeting malignant tissue of solid tumors and systemic anti-cancer effects, there is a great interest in cobalt complexes in the experimental research of malignant tumors

* Corresponding author. Inner Mongolia Key Laboratory of Mongolian Medicine Pharmacology for Cardio-Cerebral Vascular System, Tongliao, Inner Mongolia, 028000, China.

** Corresponding author. Inner Mongolia Key Laboratory of Mongolian Medicine Pharmacology for Cardio-Cerebral Vascular System, Tongliao, Inner Mongolia, 028000, China.

E-mail addresses: langzhe73@163.com (M. Zhao), qingshan_zhang666@163.com (Q.-S. Zhang).

treatment [18]. This work presents the synthesis and characterization of a dicyanamide-bridged coordination polymer $[\text{Co}(\text{L})_2(\text{dca})]_n$ by using the bidentate NO donor Schiff base (2-methoxy-6-((methylimino)methyl)phenol). Furthermore, the nanoparticles of complex **1** (denoted as nano **1** hereafter) was prepared by a green grinding approach, which has good water dispersibility. The virus burden detected by RT-PCR showed that nano **1** could significantly reduce the loading of the virus. And the values of LVEF and LVFS also suggested the obviously protective effect of nano **1** on cardiac functions. The CCK-8 assay of the nano **1** on H9C2 and HL-1 cardiomyocytes showed that the nano **1** has no toxicities on normal cells. The hypothesis that established upon the experimental observations has been examined by performing molecular docking simulation.

2. Experimental

2.1. Chemicals and measurements

The chemicals as well as reagents were purchased from Beijing Bailingwei reagent company and Tianjin Guangfu chemical reagent company, and they were utilized with no further depuration. We utilized the elemental vario micro elemental analyzer to obtain elemental results for the content of N, C, H elements content. SEM was used for the sake of depicting the configuration and morphology of the CP **1**'s nanostructures.

2.2. Preparation and characterization for coordination polymer $[\text{Co}(\text{L})_2(\text{dca})]_n$ (**1**)

We dissolved Cobalt acetate tetrahydrate which is 0.100 g and 0.4 mmol, $\text{NaN}(\text{CN})_2$ (0.036 g, 0.4 mmol) as well as Schiff base (HL) which is 0.05 g and 0.3 mmol into methanol of 10 mL. And then, we adjusted the pH numerical value of the reaction system to 5–6. Transferring and sealing up the mixture into the stainless steel container which has 25 mL Teflon-lined, heating it for 12 h at 80 °C, and then we cooled the mixture to room temperature. We acquired black single crystals suitable for X-ray diffraction analysis with block-shape. The yield was 45% (in cobalt). Elemental findings resulted to $\text{C}_{20}\text{H}_{20}\text{CoN}_5\text{O}_4$: C, 22.99; H, 4.45; N, 15.45%. Found for N: C, 23.06; H: 4.55; N: 15.72%.

The complex **1**'s X-ray data were obtained by utilizing the Oxford Xcalibur E diffractometer. The intensity data was analyzed by utilizing the CrysAlisPro software and converted to the HKL files. The SHELXS program on the basis of direct approach was utilized to create the complexes **1**'s initial structural models, the SHELXL-2014 program on the basis of the least-squares approach was modified [19]. The **1**'s whole non-H atoms were mixed with anisotropic parameters. Then we utilized the AFIX commands to fix the whole H atoms geometrically on the C atoms that they attached. Table 1 details complex **1**'s refinement details as well as crystallographic parameters.

2.3. CVB3 infection mice model

BALB/c male BALB/c mice of 6–8 weeks and 18–20 g were purchased from Model Animal Research Center of Nanjing University (Nanjing, China) and preserved under standard laboratory condition. This experiment was ratified by the Animal Protection Ethics Committee of Nanjing University. For mice infection, intraperitoneal injection (i.p.) was administered at a dose of 10^3 PFUs. CVB3 was subcultured in HeLa cells (ATCC, CCL-2). After infection, the mice were further kept in the cage with free food and water.

2.4. Real-time RT-PCR

The BALB/c male were affected by CVB3 virus, and then treated with nano **1**. On the 3rd and 7 days after infection, the loading of CVB3 virus was detected by RT-PCR accordance to the producer's plan [20]. In short, total RNA was separated by RNeasy Mini RNA Isolation Kit (QIAGEN) and quantized the concentration of RNA, followed by reverse transcript into cDNA with cDNA Synthesis Kit (Takara). Real-time PCR was performed using the SYBR Green PCR Master Mix kit (Takara). The primers were CVB3 Forward: 5'-ATCAAGTTGCGTGCTGTG-3'; CVB3 reverse: 5'-TGCGAAATGAAAGGA. The relative expression levels of CVB3 were calculated by $2^{-\Delta\Delta C_t}$ method.

2.5. Echocardiography

After infected with CVB3 virus, the mice were treated with nano **1** at the dosage of 5 mg/kg. The heart functions indicators are left ventricular fractional shortening (LVFS) and left ventricular ejection fraction (LVEF), they were evaluated by an echocardiography (Vevo2100, Visual Sonics, Canada) at the 7th day after CVB3 contagion and nano **1** treatment [21].

2.6. Toxicities detection

The toxicities of the nano **1** was detected by CCK-8 assay against cardiomyocytes H9C2 and HL-1 according to the instructions as previous introduced. In brief, the H9C2 and HL-1 cardiomyocytes were planted in 96 well plates at the final destiny of 5×10^3 cells/well, and the cells were treated with serious dilutions of nano **1** (1, 2, 4, 8, 10, 20, 40, 80 μM) with Co(II) complex used as the parallel control. After 24 h incubation at 37 °C, 5% CO_2 , 10 μL CCK8 reagent (Sigma) in 100 μL medium without FBS was added into each well for another 2 h culture. Finally, the absorbance at 450 nm was detected for each sample. The cell viability rate was calculated according to the OD450 value.

2.7. Molecular docking

In order to iterate over the conformational space of Co(II) complex when interacting with active sites provider, the stochastic

Table 1
Refinement details and crystallographic parameters for complex **1**.

Empirical formula	$\text{C}_{20}\text{H}_{20}\text{CoN}_5\text{O}_4$
Formula weight	453.34
Temperature/K	100.00(10)
Crystal system	monoclinic
Space group	C2/c
a/Å	18.0260(12)
b/Å	8.3690(5)
c/Å	14.5540(6)
$\alpha/^\circ$	90
$\beta/^\circ$	116.109(5)
$\gamma/^\circ$	90
Volume/Å ³	1971.6(2)
Z	4
$\rho_{\text{calc}}/\text{cm}^3$	1.527
μ/mm^{-1}	0.909
Reflections collected	4192
Independent reflections	1936 [$R_{\text{int}} = 0.0190$, $R_{\text{sigma}} = 0.0289$]
Data/restraints/parameters	1936/0/178
Goodness-of-fit on F^2	1.134
Final R indexes [$I \geq 2\sigma(I)$]	$R_1 = 0.0416$, $\omega R_2 = 0.1199$
Final R indexes [all data]	$R_1 = 0.0442$, $\omega R_2 = 0.1214$
Largest diff. peak/hole/e Å ⁻³	0.44/-0.86
CCDC	1947499

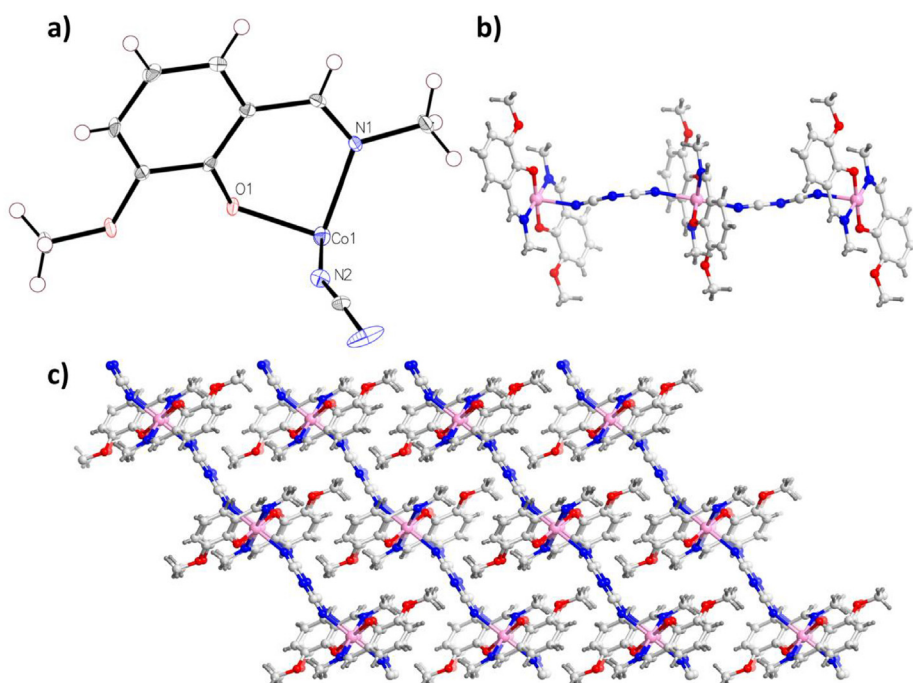


Fig. 1. (a) The basic repeating unit for **1**. (b) The **1**'s 1D chain-like network. (c) The 3D packing diagram for the network of **1**.

geometry searching approach has been used to sample through all the possible binding interactions. To address such complicated task, a modified version of autodock vina, Smina, has been used. The initial configuration of Co(II) was taken from the experimental crystal structure and used for molecular docking directly. A maximum number of 25 binding modes have been used. Visualization has been done by using open source version of PyMOL v2.3.0.

3. Results and discussion

3.1. Molecular structure

The Schiff base ligand (2-methoxy-6-((methylimino)methyl)phenol) could be prepared by refluxing an excess MeNH₂ with the 2-hydroxy-3-methoxybenzaldehyde in the MeOH solution. After slow evaporation of the reaction mixture, a bright yellow crystalline solid of HL was obtained in a 60% yield. Reaction of cobalt acetate tetrahydrate, HL and NaN(CN)₂ in the MeOH solution under the solvothermal condition results in forming the targeted complex **1** with a moderate high productivity. The refinement results as well as structural solution on the basis of the crystal data collected at 100 K reflected that the black crystals of **1** is part of the monoclinic crystal system that the space group is C2/c and demonstrates a 1D chain-like network. Complex **1**'s asymmetric unit is shown in Fig. 1, which indicates that the neutral network of **1** is composed of one half Co(II) ion located on the 2-fold crystallographic axis, one deprotonated L ligand along with a half HN(CN)₂ molecule. Similar to the reported complex on the basis of the L ligand, the Co²⁺ ion takes up the N2O2 donor chamber of two L⁻ ligands. Two phenoxo oxygen atoms (O1 and O1A) as well as two imine nitrogen atoms (N1 and N1A) can coordinate the Co²⁺ ion, and it forms the base of a square pyramid, while N2 of μ_{1,5}-bidentate dca takes up the top coordination. The Co–O bond distance is 1.854(2) Å and the bond lengths of Co–N are in the region of 2.036(8) to 2.293(18), which are comparable with those Co–O and Co–N bond distances in the reported document [22]. The dca ligand, which adopts a μ_{1,5}-bidentate bridging mode, connects with the adjacent CoL₂ units

along the b axis to afford a 1D layered network with the Co–Co separation of 8.744 Å (Fig. 1b). Further research to the framework shows that there are without π–π interactions in the formed 1D chain-like network. However, using the calcd H-bond manipulation embedded in the software PLATON, there still exist the non-classic H-bond interaction in the 1D chains, which is formed by the H atom on the C8 and the O1 atom with the C–H···O distance of 2.858 Å. The packing of the 1D chain-like structure via the Van der Waals force affords a tightly packing 3D supramolecular framework with no accessible solvent free volume (Fig. 1c). To check the phase purity of the as-prepared **1**, its PXRD patterns were collected using the freshly as-prepared samples at room temperature. As shown in Fig. S1, the PXRD pattern of the as-synthesized **1** is almost identical to the calculated pattern, indicating the as-prepared **1** shows high phase purity.

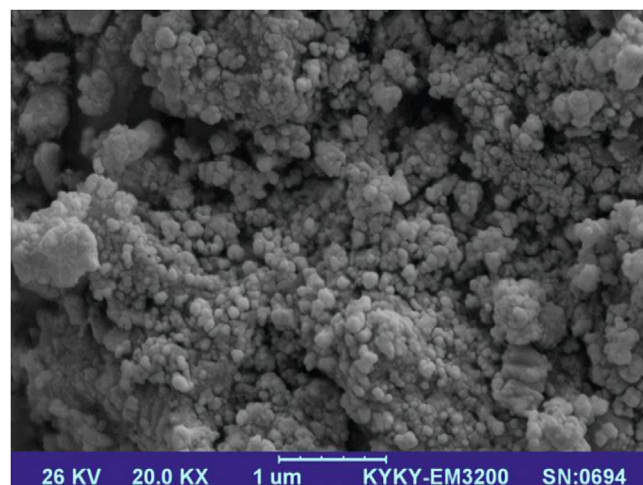


Fig. 2. The SEM micrograph for the nanoparticles of **1**.

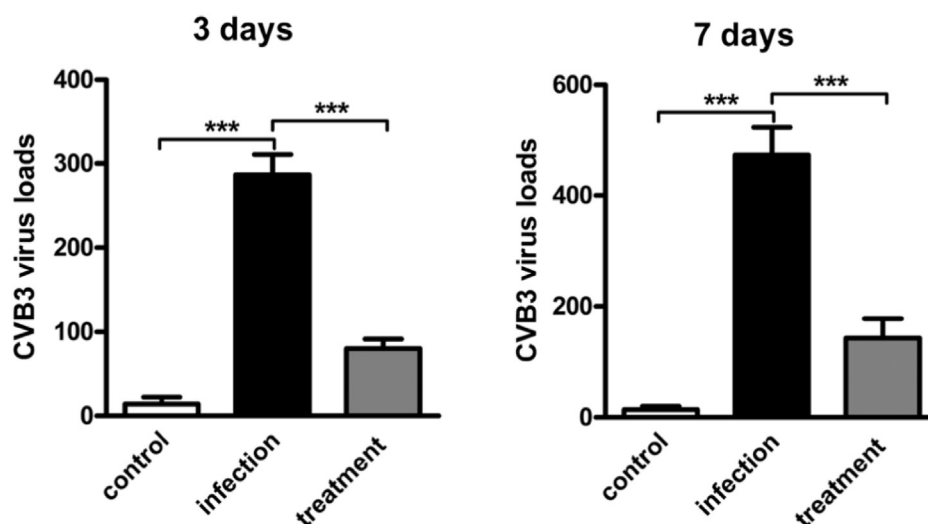


Fig. 3. Protective effect of nano **1** on mice infected with CVB3 virus. The infection of BALB/c with CVB3 virus and given nano **1** for treatment. the loads of CVB3 virus in mice was measured by RT-PCR, $p < 0.05$ was considered as obvious difference. This experiment was in triplicate.

3.2. Preparation of the nanostructure of **1**

Considering the following bioactivity tests, it is essentially reducing the particle size of **1** to the nanometer scale, which can motivate the drug to be discharged into the whole body and then can be absorbed by specific tissues through the intravenous administration. In the previous studies, it has been shown that the mechanical grinding technology is a green and valid approach to establish coordination polymer nanostructures that are simple to be operate. Intriguingly, for the complex **1**'s single crystals, the crystalline nanoscale complex **1** were acquired when the single crystals were mechanically ground in a pestle and mortar for approximately 30 min. The crystalline nature of the nanoscale materials is confirmed by PXRD studies, and it is also noticed that the PXRD pattern of the nanoscale compound matched perfectly well with the simulated and bulk PXRD patterns of the complex **1**, indicating complex **1** could maintain the integrity after the formation of the nanoparticles (Fig. S1) [23,24]. The nanostructures' formation was further identified by utilized SEM studies, which were acquired by dropping the nanostructures' DMSO dispersion

solution on the surface of a glass, and the thickness for the ball-like nanoparticles is around 186 nm for nanostructure **1** (Fig. 2). The as-prepared nanostructure has good dispersibility in the aqueous solution (Fig. S2).

3.3. Nano **1** reduces the CVB3 virus burden in mice

Coxsackie virus B3 (CVB3) is a globally prevalent virus, which is frequently associated with myocarditis. As reported, most myocarditis diseases were caused by CVB3 virus infection. So, to further explore the protective effect nano **1** in the CVB3 infected animal model, the animal model was constructed firstly followed by the nano **1** treatment. Then, the virus burden was measured by RT-PCR assay. As the results showed in Fig. 3, the virus loads on the 3rd and 7th day after treatment was significantly reduced in a time-dependent manner. The nano **1** could reduce the loads to 20% and 25%, compared to the infection model group ($p < 0.005$). This result suggested the nano **1** could significantly reduce the virus in the infected animal, and exert an excellent protective effect in vivo.

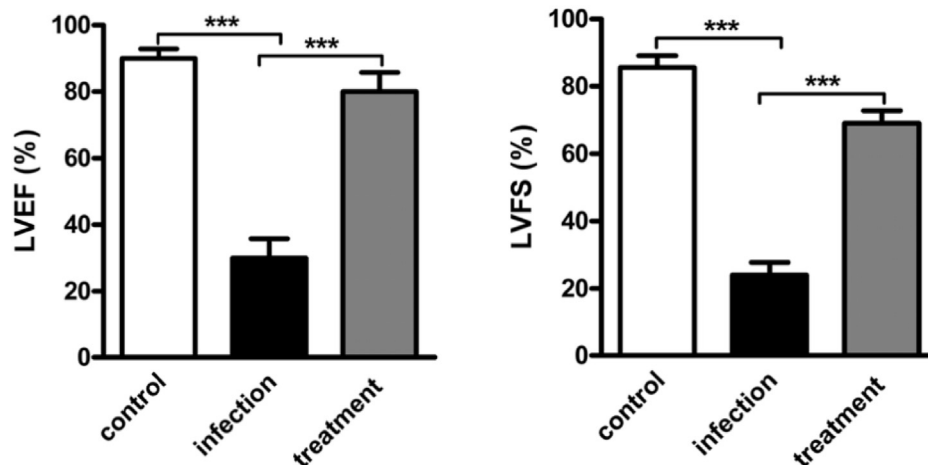


Fig. 4. Increased cardiac functions of CVB3 virus infected mice after nano **1** treatment. The CVB3 virus infected mice were given complexes for 7 days treatment, the cardiac functions were evaluated by LVEF and LVFS. $p < 0.05$ was considered as obvious difference, this study was repeated at least three times. Nano **1** showed no toxicities on H9C2 and HL-1 cardiomyocytes.

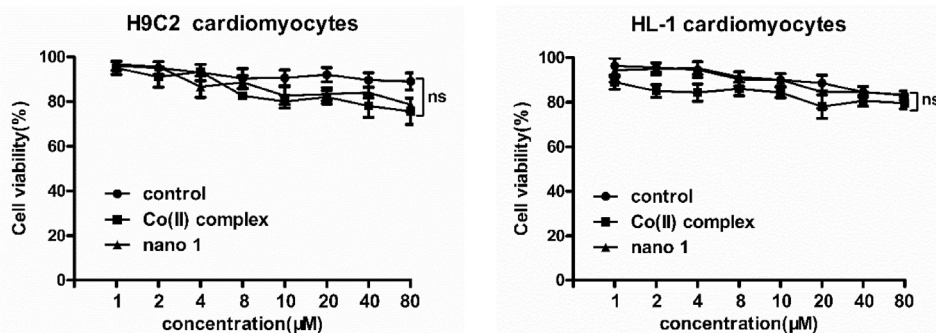


Fig. 5. No toxicities of nano 1 on H9C2 and HL-1 cardiomyocytes. The H9C2 and HL-1 cardiomyocytes were treated with serious dilutions of nano 1 for 24 h, the toxicities of nano 1 on H9C2 and HL-1 cardiomyocytes was evaluated by CCK-8 assay. This experiment was conducted at least three times.

3.4. Nano 1 improve the cardiac functions of CVB3 virus infected mice

Myocarditis is combined with LVEF and LVFS systolic dysfunction, which are applied in the diagnosis, management and prognostication of myocarditis. During the procession of myocarditis, there is usually a reduced level of LVEF and LVFS compared with the normal people. As the important marker of cardiac functions, the LVEF and LVFS of CVB3 virus infected mice was evaluated at the end of the nano 1 treatment period. We can see, the CVB3 virus infection caused a weaker left ventricular systolic function, the percentage of LVEF was reduced to about 30%, but this damage could be reversed by nano 1 to almost 80% obviously (Fig. 4). This result suggested the excellent protective effect of nano 1 on the cardiac functions of CVB3 virus infected mice.

Considering the necessary of nano 1 willing to become a drug, the toxicities of the nano 1 on H9C2 and HL-1 cardiomyocytes was evaluated by CCK-8 assay. The H9C2 and HL-1 cardiomyocytes were treated with serious dilutions of nano 1 (1, 2, 4, 8, 10, 20, 40, 80 μM), using Co(II) complex as the parallel control in this experiment for 24 h. As results showed in Fig. 5, nano 1 didn't affect the cell viability of both H9C2 and HL-1 cardiomyocytes, the cell viability rate were still over 80% after 24 h treatment. These results indicated that the nano 1 showed no toxicities on H9C2 and HL-1 cardiomyocytes, it's protective effect on CVB3 virus infected mice was due to the reducing of the virus burden and improving of the cardiac functions.

3.5. Molecular docking

Generally, the drug-like or protective features of the ligand are the capabilities of interacting with double helix structure from DNA or residues from protein, because most diseases are caused by the cleavage of double helix structure or the conformation changing of protein. Molecular docking approach is a tool that could help us to reveal how ligand interacts with either DNA or protein at the molecular level. To understand the experimental phenomenon observed by the experimental results described above, the protein 4QJU (PDBID) has been chosen to probe the possible interactions between Co(II) complex, the advantage of using 4QJU as the receptor is that the structure contains both double helix structure and residues that belong to common protein. Furthermore, 4QJU is a widely used target protein for metallic complexes for cytotoxicity studies including but not limited to Co(II), Zn(II) and Mn(II) [25,26], so it is a suitable receptor for the myocarditis study of synthesized Co(II) complex in the current study. The docking pocket that provided by 4QJU is formed between DNA and protein structures, the length of the docking grid is set to 22.5 Å which is large enough to

cover the entire docking pocket, and 25 docking trials were used for the screening of the possible binding interactions. The Co(II) complex can be used as protective activity with strong confidence due to the activity to interact with both DNA and protein, as shown in Fig. 6a, which depicts the summary view of Co(II) complex wrapping into the binding pocket that was provided by 4QJU. The molecular docking results show that 8 different binding modes has been found above the 25 searches, the binding energies are increasing from -6.2 to -3.4 kcal/mol. In Fig. 6b and c we show two energy favorable binding modes in which the chain structures of nitrogen are interacting with double helix structure on the one hand and with protein on the other hand. While the energy unfavorable binding mode is showing that the stability of the binding is weak when oxygen-containing functional groups are interacting with the receptor. Such result has qualitative agreement to the observations in experiment.

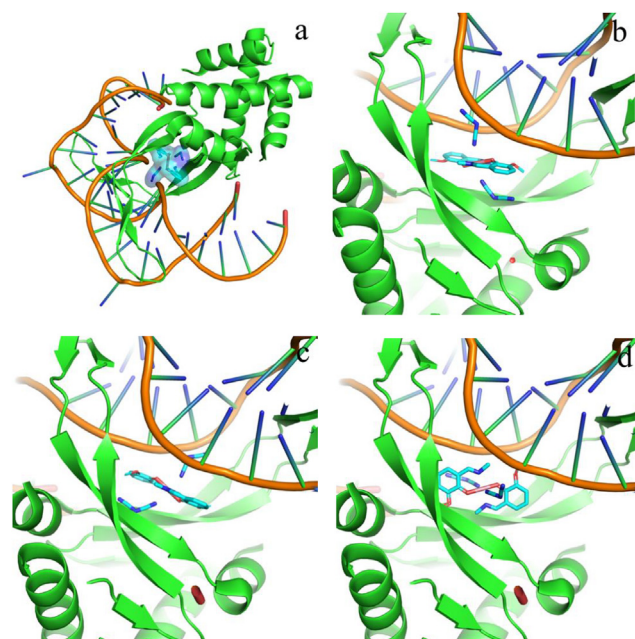


Fig. 6. The summary view of the molecular docking of Co(II) complex with receptor protein (4QJU) (a), two most favorable binding modes that were found during the molecular docking, their association binding energies are -6.2 (b) and -6.0 (c) kcal/mol, the energy unfavorable binding mode (d) with its highest binding energy of -3.4 kcal/mol among all other 7 possibilities.

4. Conclusion

In summary, a dicyanamide-bridged coordination polymer has been successfully prepared by using the bidentate NO donor Schiff base ligand (2-methoxy-6-((methylimino)methyl)phenol under the solvothermal conditions. The structure of the as-prepared complex **1** have been characterized by single crystal X-ray diffraction studies, which demonstrates that complex **1** has a rod-like 1D chain bridged by DCA, among it the Co(L)₂ units are bridged by dca ligands along the a axis. Furthermore, the nanoparticles of complex **1** were prepared by a green grinding approach, which has good water dispersibility. We constructed the in vivo mice model successfully, then we measured the inhibitory effect of nano **1** on mice virus loads. Next, the cardiac functions of mice were also detected to evaluate the cardiac functions after nano **1** treatment. All the results in this study suggested the nano **1** could reduce the virus burden and improve the cardiac functions, it has excellent protective effect in CVB3 virus infected mice. The most important the nano **1** showed no toxicities on H9C2 and HL-1 normal cardiomyocytes, which is detected by CCK-8 assay. Molecular docking results show that the chain structures of nitrogen on the Co(II) could improve the stability of binding interactions between ligand and receptor while oxygen-containing functional groups have negative influence on the binding interaction, while reveals the protective activity mechanism from the molecular level.

Acknowledgment

This work was supported by grants from Research Projects of Institutions of Higher Learning in Inner Mongolia (NJZY17195) and Inner Mongolia Natural Science Foundation [2017MS(LH)0824].

Appendix A. Supplementary data

Supplementary data to this article can be found online at

<https://doi.org/10.1016/j.molstruc.2019.127038>.

References

- [1] C. Tschöpe, L.T. Cooper, G. Torre-Amione, S. Van Linthout, *Circ. Res.* 124 (2019) 1568.
- [2] L. Kang, L. Zhao, S. Yao, C. Duan, *Ceram. Int.* 45 (2019) 16717.
- [3] Y. Liu, X. Huang, Y. Liu, D. Li, J. Zhang, L. Yang, *Exp. Ther. Med.* 17 (2019) 4471.
- [4] C. Duan, F. Li, M. Yang, H. Zhang, Y. Wu, H. Xi, *Ind. Eng. Chem. Res.* 57 (2018) 15385.
- [5] J. Beuy, V. Wiwanitkit, *Anatol. J. Cardiol.* 21 (2019) 293.
- [6] Y.Y. Yang, L. Kang, H. Li, *Ceram. Int.* 45 (2019) 8017.
- [7] X. Feng, Y.Q. Feng, J.L. Chen, L.Y. Wang, *Dalton Trans.* 44 (2015) 804.
- [8] C. Duan, J. Huo, F. Li, M. Yang, H. Xi, *J. Mater. Sci.* 53 (2018) 16276.
- [9] X. Feng, L.F. Ma, L. Liu, S.Y. Xie, L.Y. Wang, *Cryst. Growth Des.* 13 (2013) 4469.
- [10] H. Zhang, Y. Fang, *J. Alloy. Comp.* 781 (2019) 201.
- [11] X. Feng, L.Y. Wang, J.-S. Zhao, J.G. Wang, S.W. Ng, B. Liu, X.G. Shi, *CrysEngComm* 12 (2010) 774.
- [12] X. Feng, J.S. Zhao, B. Liu, L.Y. Wang, J.G. Wang, S.W. Ng, G. Zhang, X.G. Shi, Y.Y. Liu, *Cryst. Growth Des.* 10 (2010) 1399.
- [13] A.K. Patel, R.N. Jadeja, H. Roy, R.N. Patel, S.K. Patel, R.J. Butcher, *J. Mol. Struct.* 1185 (2019) 341.
- [14] B. Barszcz, J. Masternak, M. Hodorowicz, E. Matczak-Jon, A. Jabiońska-Wawrzycka, K. Stadnicka, M. Zienkiewicz, K. Królewska, J. Kaźmierczak-Barańska, *Inorg. Chim. Acta* 399 (2013) 85.
- [15] N. Alvarez, L.F.S. Mendes, M.G. Kramer, M.H. Torre, A.J. Costa-Filho, J. Ellena, G. Facchin, *Inorg. Chim. Acta* 483 (2018) 61.
- [16] A.C. Hangan, G. Borodi, R.L. Stan, E. Páll, M. Cenariu, L.S. Oprean, B. Sevastre, *Inorg. Chim. Acta* 482 (2018) 884.
- [17] D.S. Raja, N.S.P. Bhuvanesh, K. Natarajan, *Dalton Trans.* 41 (2012) 4365.
- [18] B.F. Long, Q. Huang, S.L. Wang, Y. Mi, M.F. Wang, T. Xiong, S.C. Zhang, X.H. Yin, F.L. Hu, *J. Coord. Chem.* 72 (2019) 645.
- [19] G.M. Sheldrick, *Acta Crystallogr. Sect. C Struct. Chem.* 71 (2015) 3.
- [20] X. Yang, Y. Yue, S. Xiong, *Front. Cell. Infect. Mi.* 9 (2019) 57.
- [21] L. Zhao, L. Kang, S. Yao, *IEEE Access* 7 (2019) 984.
- [22] M.Y. Sun, D.M. Chen, *Inorg. Chem. Commun.* 82 (2017) 61.
- [23] S. Mukherjee, S. Ganguly, K. Manna, S. Mondal, S. Mahapatra, D. Das, *Inorg. Chem.* 57 (2018) 4050.
- [24] T. Kundu, S. Mitra, P. Patra, A. Goswami, D. Díaz Díaz, R. Banerjee, *Chem.-A Eur. J.* 20 (2014) 10514.
- [25] E. Gao, J. Xing, Y. Qu, X. Qiu, M. Zhu, *Appl. Organomet. Chem.* 32 (2018) e4469.
- [26] M. Zhu, H. Zhao, T. Peng, J. Su, B. Meng, Z. Qi, B. Jia, Y. Feng, E. Gao, *Appl. Organomet. Chem.* 33 (2018), e4734.